The cysteines of the extracellular loop are crucial for trafficking of human organic cation transporter 2 to the plasma membrane and are involved in oligomerization

Sabine Brast[*], **Alexander Grabner**[*], **Sonja Sucic**[†], **Harald H. Sitte**[†], **Edwin Hermann**[‡], **Hermann Pavenstädt**[*], and **Eberhard Schlatter**[*], and **Giuliano Ciarimboli**[*,1]

[*]Medizinische Klinik und Poliklinik D, Experimentelle Nephrologie, Universitätsklinikum Münster, Münster, Germany

[‡]Klinik und Poliklinik für Urologie, Universitätsklinikum Münster, Münster, Germany

[†]Institut für Pharmakologie, Medizinische Universität Wien, Vienna, Austria

Abstract

Human organic cation transporter 2 (hOCT2) is involved in transport of many endogenous and exogenous organic cations, mainly in kidney and brain cells. Because the quaternary structure of transmembrane proteins plays an essential role for their cellular trafficking and function, we investigated whether hOCT2 forms oligomeric complexes, and if so, which part of the transporter is involved in the oligomerization. A yeast 2-hybrid mating-based split-ubiquitin system (mbSUS), fluorescence resonance energy transfer, Western blot analysis, cross-linking experiments, immunofluorescence, and uptake measurements of the fluorescent organic cation 4-(4-(dimethylamino) styryl)-*N*-methylpyridinium were applied to human embryonic kidney 293 (HEK293) cells transfected with hOCT2 and partly also to freshly isolated human proximal tubules. The role of cysteines for oligomerization and trafficking of the transporter to the plasma membranes was investigated in cysteine mutants of hOCT2. hOCT2 formed oligomers both in the HEK293 expression system and in native human kidneys. The cysteines of the large extracellular loop are important to enable correct folding, oligomeric assembly, and plasma membrane insertion of hOCT2. Mutation of the first and the last cysteines of the loop at positions 51 and 143 abolished oligomer formation. Thus, the cysteines of the extracellular loop are important for correct trafficking of the transporter to the plasma membrane and for its oligomerization.—Brast, S., Grabner, A., Sucic, S., Sitte, H. H., Hermann, E., Pavenstädt, H., Schlatter, E., and Ciarimboli, G. The cysteines of the extracellular loop are crucial for trafficking of human organic cation transporter 2 to the plasma membrane and are involved in oligomerization.

Keywords

hOCT2; site-directed mutagenesis; regulation

The human organic cation transporter 2 (hOCT2), together with its paralogs hOCT1 and hOCT3, belongs to the SLC22 family of membrane transporters. OCT1, OCT2, and OCT3 are mainly expressed in epithelia of intestine, liver, brain, and kidney in a species- and paralog-specific fashion (1). These transporters have important physiological, pharmacological, and toxicological implications because of their role in the transport of endogenous and exogenous organic cations. Specifically, hOCT2 transports the dopaminergic neuromodulators histidyl-proline diketopiperazine and salsolinol (2), histamine (3), and xenobiotica, such as metformin (4, 5), platin derivatives (6–9), ifosfamide (10), and paraquat (11). The high expression of hOCT2 in the dopaminergic brain region of the substantia nigra (2), and in the proximal tubules (PTs) of the kidney (12), where renal dopamine is produced (13), suggests that this transporter has a crucial importance in modulating cerebral and renal dopaminergic activity. Dopamine is one of the major natriuretic factors and plays a pivotal role in Na^+ homeostasis and blood pressure regulation (13). This fact, together with the notion that OCT2 is also part of the classical uptake 2 system of stress hormone inactivation by uptake of catecholamines, which are able to initiate the reninangiotensin-aldosterone cascade and control vascular resistance (14), underlines the great potential pathophysiological importance of hOCT2 as a candidate gene for hypertensive disorders. Indeed, single-nucleotide polymorphisms (SNPs) of hOCT2 seem to be related to patient sensitivity to hypertension (14, 15). Considering the high expression of hOCT2 in the kidney, where it is localized on the basolateral membrane of PT cells, and considering that, chemically, more than half of the prescribed drugs are positively charged and belong to the group of organic cations (16), it is evident that the function of this transporter has also important pharmacological implications.

The transport mediated by OCTs has been characterized as polyspecific, bidirectional, and electrogenic (17). Common structural properties of OCTs are the presence of 12 putative α-helical transmembrane domains (TMDs) with a large hydrophilic extracellular loop bearing multiple glycosylation sites between TMD1 and TMD2 and a big intracellular loop between TMD6 and TMD7 containing several potential protein kinase phosphorylation sites (18). Despite the increasing number of studies reporting OCT function and regulation, much less information is available regarding the mechanisms involved in the cellular processing of this transporter, such as oligomer formation. Oligomerization is known to occur in many membrane proteins, and the importance of this process is just beginning to be appreciated. One documented role for oligomer formation is to facilitate passage through the tightly controlled quality control system of the endoplasmic reticulum (ER; ref. 19). Oligomerization of membrane proteins appears to be essential for transport from the ER to the plasma membrane. Whether oligomerization of transport proteins also plays a functional role in substrate transport is not yet clear; many membrane proteins seem to be functionally competent as monomers, despite their participation in oligomer assembly (20). Such information is lacking for all organic cation transporters. Therefore, we investigated the possibility of whether hOCT2, the key paralog in human kidney and brain, is able to form oligomeric complexes and which part of the transporter is involved in the oligomer formation. With several approaches, such as a yeast 2-hybrid mating-based split-ubiquitin system (mbSUS), fluorescence resonance energy transfer (FRET) analysis, chemical cross-linking, Western blot analysis, immunofluorescence, and functional transport studies, we

were able to show that hOCT2 is, indeed, able to form oligomers. The process of oligomerization seems to be important for the insertion of the transporter in the membrane. The transporter domain critical for oligomerization seems to be the large extracellular loop, where 6 cysteines determine the correct folding of the loop, and therefore the interaction of hOCT2 monomers.

MATERIALS AND METHODS

Cell culture and transfection

Human embryonic kidney 293 (HEK293) cells (CRL-1573; American Type Culture Collection, Rockville, MD, USA) and HeLa SS6 cells were grown in DMEM supplied with 10% FCS, 1% penicillin/streptomycin, 2.0 mM L-glutamine and, only for the stably transfected OCT-HEK293 cells, 0.8 mg/ml geneticin (21) at 37°C and 8% CO_2. Transient transfections were performed 24 h after cells were seeded with the specific DNA constructs using Lipofectamine (Invitrogen, Karlsruhe, Germany).

DNA constructs and mutagenesis

The full-length hOCT2 (SLC22a2, NM 003058) cloned in the expression vector pRc/CMV was kindly provided by Hermann Koepsell (University of Würzburg, Würzburg, Germany). To obtain the hOCT2 mutants C51A, C63A, C89A, C103A, C122A, and C143A, each of the cysteines of the big extracellular loop was individually mutated to alanine. Furthermore, 2 control mutations of hOCT2 were created by mutating a glycine of the extracellular loop at position 120 (G120A) and a further cysteine residue at position 179 (C179A), which is not located in the extracellular loop, to alanine. All mutations were accomplished by using the quick-change site-directed mutagenesis kit (Stratagene, La Jolla, CA, USA) following the instructions of the manufacturer and using the primers listed in Supplemental Table S1.

For fluorescence analysis, the hOCT2 and mutated clones were amplified by PCR and cloned in the plasmids pEGFP-N3, pYGFP-C1 or N1, and pECFP-N1 or C1 (Clontech-Takara Bio Europe, Saint-Germain-en-Laye, France) to obtain GFP-, YFP-, or CFP-tagged constructs. The primers used are listed in Supplemental Table S2. All constructs were verified by automated sequencing.

Yeast 2-hybrid mbSUS

This system allows *in vivo* cloning of PCR products by recombination into expression vectors, mating-based detection of the interactions, and improved selection of interacting fusions on medium lacking histidine and adenine (22, 23). The mbSUS is based on the observation that the N-terminal ubiquitin (Nub) domain can reconstitute a full-length ubiquitin protein when coexpressed with the C-terminal ubiquitin (Cub) half. In mbSUS, the reconstituted ubiquitin is recognized by ubiquitin-specific proteases (USPs), which release the artificial transcription factor protein A-LexA-VP16 (PLV) fused to the C-terminus of Cub. The released PLV diffuses into the nucleus and activates a set of reporter genes. The mbSUS assay was performed according to the protocol previously described (22, 23). Briefly, the full-length hOCT2 linked with B1 and B2 site hOCT2 was fused to the Cub-PLV fragment into pMetYCgate (bait) vector *via in vivo* cloning and transformed in the

haploid yeast strain THY.AP4 (MAT a). The full-length B1- and B2-linked hOCT2 was also fused to the NubG fragment into pNXgate (prey) and transformed in the haploid yeast strain THY.AP5 (MAT α, *in vivo* cloning). NubG is a Nub mutant that has reduced affinity for Cub and can reconstitute the full-length ubiquitin only when brought into its proximity *via* interacting proteins. Before mating, the correct expression of transporter proteins was verified in the haploid yeast strains by Western blot analysis using antibodies against hOCT2 (not shown). After mating of the hOCT2-Cub and NubG-hOCT2 protein-expressing yeast cells, the presence of plasmids was assayed by growth on appropriate selection medium. Yeast cells containing both plasmids were then inoculated on plates with medium lacking essential amino acids. Only yeast cells in which reporter genes for histidine and adenine were activated through interaction of the Cub- and NubG-fused hOCT2 proteins were able to grow. After a few days, growth was detected on the selective interaction medium for the hOCT2-expressing yeast cells. Positive control experiments, where the hOCT2-Cub proteins were expressed with a wild-type (WT) Nub protein, were performed in parallel. Since the WT Nub fragment spontaneously associates unspecifically with the Cub fragment of the hOCT2, strong growth was observed. To exclude false-positive results, 2 independent negative control experiments were performed. First, to exclude a self-activating process, the interaction of the hOCT2-Cub proteins was tested with an empty NubG plasmid, where only the NubG fragment is expressed. Second, to assure the specificity of the reaction, the interaction of hOCT2-Cub proteins with NubG-fused vacuolar type H^+-ATPase (VATPase) protein, which was shown not to be an interacting partner of hOCT2, was also tested. The primers used in the mbSUS are listed in Supplemental Table S3.

FRET

FRET signals were measured with an epifluorescence microscope (Axiovert 200; Carl Zeiss, Oberkochen, Germany) using the 3-filter method according to Xia and Liu (24). For oligomerization studies of hOCT2, the N- and C-terminal CFP- and YFP-tagged transporter proteins were cotransfected in HEK293 cells. Briefly, HEK293 cells were seeded onto poly-D-lysine-coated glass coverslips. The next day, cells were transiently transfected with different constructs using the calcium phosphate precipitation method: 1–3 μg of cDNA was mixed with $CaCl_2$ and HBS buffer (in mM: 280 NaCl, 10 KCl, 1.5 Na_2HPO_4, 12 dextrose, and 50 HEPES); after 6–10 min, the calcium phosphate-DNA precipitate was added to the cells. After 4–5 h, the cells were washed twice with PBS and briefly treated with glycerol, followed by the addition of FCS-containing medium. Medium was replaced by Krebs-HBS buffer (in mM: 10 HEPES, 120 NaCl, 3 KCl, 2 $CaCl_2$, and 2 $MgCl_2$), and images were taken using a microscope equipped with a ×63 oil objective and a Ludl filter wheel that allows for rapid exchange of filters (Ludl Electronic Products, Hawthorne, NY, USA). The system was equipped with the following fluorescence filters: CFP filter (I_{CFP}; λ_{ex}=436 nm, dichroism=455 nm, λ_{em}=480 nm), YFP filter (I_{YFP}; λ_{ex}=500 nm, dichroism=515 nm, λ_{em}=535 nm), and FRET filter (I_{FRET}; λ_{ex}=436 nm, dichroism=455 nm, λ_{em}=535 nm). Acquisition of the images was done with MetaMorph 4.6. (Molecular Devices Corp., Downingtown, PA, USA). Background fluorescence was subtracted from all images, and fluorescence intensity was measured at the plasma membrane and in cytosolic regions in all images. To calculate a normalized FRET signal (N_{FRET}), we used the following equation:

$$N_{\text{FRET}} = \frac{I_{\text{FRET}} - a \times I_{\text{YFP}} - b \times I_{\text{CFB}}}{\sqrt{I_{\text{YFP}} \times I_{\text{CFP}}}}$$

where *a* and *b* represent the bleedthrough values for YFP and CFP. Corrected FRET (FRETc) images were obtained according to Xia and Liu (24). Briefly, after background subtraction from all three images, CFP and YFP images were multiplied by their corresponding bleedthrough values. The following equation was used for the calculation of FRETc images: FRETc = FRET – (*b* × CFP) – (*a* × YFP). FRET signals were calculated and displayed with ImageJ PixFret software (ref. 25; http://rsb.info.nih.gov/ij/).

Two positive controls were used in each experiment: a CFP-YFP fusion protein and serotonin transporter (SERT) with CFP and YFP tags as its N and C termini, respectively. SERT has been shown to homooligomerize by FRET microscopy and biochemical approaches (26). Negative control experiments included coexpression of CFP and YFP or the coexpression of hOCT2-CFP and Pal-Myr-YFP, a YFP construct with a signal sequence tethering the YFP moiety to the plasma membrane.

Cross-linking experiments

The sulfhydryl-specific cross-linker 1,8-*bis*-(maleimido)diethylene glycol [BM(PEG)$_2$] with a spacer arm of 14.7 Å (Thermo Scientific, Rockford, IL, USA) was used in cross-linking experiments. A 20 mM BM(PEG)$_2$ stock solution in DMSO was freshly prepared immediately before use. The stock solution was diluted in 1% Triton X-100 in PBS to get a 2.5 mM working solution, which was used as lysis buffer. Confluent HEK293 cells transfected with hOCT2 or the mutated transporters were washed twice with ice-cold PBS, collected from the well with 1 ml ice-cold PBS, and pelleted by centrifugation (2400 *g*, 5 min at room temperature). Pellets were resuspended in the cross-linker containing lysis buffer and incubated for 45 min in the dark at room temperature. The reaction was quenched with the addition of NuPAGE LDS 4× LDS sample buffer (Invitrogen) for 10 min. Samples were heated at 50°C for 30 min and analyzed by SDS-PAGE and Western blot analysis.

Western blot analysis and SDS-PAGE

For Western blot analysis, human kidney cortex was homogenized in lysis buffer (10 mM Tris-HCl, pH 7.5), and hOCT2-HEK293 cells were osmolyzed in the same buffer. To avoid protein aggregations, protein samples were not boiled. The lysates were centrifuged for 1 min at 10,000 *g* to remove cell debris. The supernatant was centrifuged again (20,000 *g* for 1 h). Supernatants of renal cortex and HEK293 cells were diluted 4-fold with sample buffer with (Roti-Load 1; Roth, Karlsruhe, Germany) or without (Roti-Load 2; Roth) reducing agents, incubated 15 min at 50°C, and transferred to polyvinylidene fluoride (PVDF) membrane for Western blot analysis. The membranes were blocked with 3% gelatin from coldwater fish skin (Sigma, Munich, Germany). After incubation with the primary antibody (anti-hOCT2, as described in ref. 21) at 1:500 dilution, membranes were incubated with peroxidase-conjugated anti-mouse (Dako Deutschland, Hamburg, Germany) at 1:10,000 dilution. Signals were visualized by West-Zol plus Western blot detection system (iNtRON Biotechnology, Seongnam, Korea). For deglycosylation experiments, lysates from hOCT2-

expressing HEK293 cells were treated with PNGase F (New England BioLabs, Ipswich, MA, USA), according to the manufacturer's protocol.

Immunocytochemistry

HeLa SS6 cells transiently transfected with tagged hOCT2 or tagged hOCT2 mutants (see DNA Constructs and Mutagenesis) grown on coverslips were fixed in PBS containing 4% paraformaldehyde (PFA) for 10 min. After fixation, the cells were washed 3 times with Dulbecco's PBS (Biochrom, Berlin, Germany) and incubated with 0.1% Triton X-100 for 3 min. After extensive washing with PBS, unspecific binding sites were blocked by overnight incubation at 4°C with 10% BSA (Sigma) in PBS. Cells were then incubated for 60 min at room temperature with anti-calnexin or anti-GM130 antibodies (BD Biosciences, Heidelberg, Germany) diluted 1:1000 in 1% BSA in PBS. After 3 washing steps in PBS, the secondary antibody (goat-anti-mouse Alexa Fluor 594; Invitrogen) at 1:1000 dilution was incubated for 60 min, followed by 5 more washing steps in PBS. Finally, cells were covered with Fluoromount (Sigma), and fluorescence photographs were taken with an Axiocam camera mounted on an Axiovert 100 microscope using Axiovision software (Carl Zeiss).

Isolation of PTs from human kidney

Human kidney samples were obtained from patients undergoing tumor nephrectomy. The procedure was approved by the ethics commission of the Universitätsklinikum Münster, and written consent was obtained from the patients. A piece of normal kidney tissue surrounding the tumor was transferred into chilled HCO_3^--free phosphate buffer immediately after nephrectomy. S3 segments of PTs of human kidney samples were isolated mechanically with fine forceps in DMEM culture medium containing 5 mM albumin at 4°C, as described previously (27). Tubule segments were transferred to the perfusion chamber and fixed between 2 glass holding pipettes for transport measurements.

Fluorescence measurements with 4-(4-(dimethylamino)styryl)-*N*-methylpyridinium (ASP⁺)

As substrate for organic cation transport in hOCT2-expressing HEK293 cells or in freshly isolated human PTs, the fluorescent organic cation ASP⁺ at a concentration of 1 μM was used, as already published (28, 29). For uptake measurements, HEK293 cells were seeded in 96-well plates. After 24 h, the cells were transfected with 0.3 μg plasmid DNA/well using Lipofectamine (Invitrogen). ASP⁺ uptake by hOCT2 and hOCT2 mutants was measured at 24–48 h after transfection by using a fluorescent plate reader (Infinity M200; Tecan, Crailsheim, Germany), as described previously (30). ASP⁺ uptake across the basolateral membrane of isolated human tubules was measured in the dark by dynamic fluorescence microscopy with an inverted microscope (Axiovert 135; Carl Zeiss) equipped with a ×100 1.45 oil-immersion objective, as previously described (27, 30). As superfusion solution, a HCO_3^--free, Ringer-like solution was used (in mM: 145 NaCl, 1.6 K_2HPO_4, 0.4 KH_2PO_4, 5 D-glucose, 1.3 calcium gluconate, and 1 $MgCl_2$, pH adjusted to 7.4). In all fluorescence measurements, the initial linear slope of cellular fluorescence increase after ASP⁺ addition was used as transport parameter (31). To examine whether the disulfide bonds play a role in the transport function of hOCT2, hOCT2-transfected cells or PTs freshly isolated from human kidneys were incubated with increasing concentrations of the reducing agent dithiothreitol (DTT) for 10 min, followed by the measurement of ASP⁺ uptake. The apparent

affinity (IC_{50}) of the prototypical organic cation tetraethylammonium (TEA^+) for the ASP^+ uptake was also determined in hOCT2-HEK293 cells with or without 10 min incubation with 20 mM DTT.

Chemicals

ASP^+ was purchased from Molecular Probes (Leiden, The Netherlands). All other substances and standard chemicals were obtained from Sigma or Merck (Darmstadt, Germany).

Statistical analysis

Data are presented as means ± SE, with *n* referring to the number of cell monolayers or isolated tubules used in the experiments. Unpaired 2-sided Student's *t* test and ANOVA (with Tukey *post hoc* test) were used to prove statistical significance of the effects. A value of $P < 0.05$ was considered statistically significant. Statistical analysis and calculation of IC_{50} were performed using GraphPad Prism 5.0 (GraphPad Software Inc., San Diego, CA, USA).

RESULTS

Interaction of hOCT2 proteins in the mbSUS

Results obtained with mbSUS identified significant interaction of hOCT2 with itself and provided evidence that hOCT2 polypeptides are capable of coassembling in a homomeric protein complex. A representative picture of yeast growing on minimal medium on hOCT2-hOCT2 interaction in the mbSUS is given in Fig. 1.

Oligomerization analyzed by FRET in living cells

FRET technology is frequently used for the investigation of protein-protein interactions because the energy transfer between 2 interacting proteins is only possible when the molecules are in proximity (Foerster distance for CFP-YFP <50 Å) and have an appropriate relative orientation. Because the main fluorescence signals of the hOCT2 proteins were observed at the plasma membrane (Fig. 2*A*), the region of interest selected for the calculation of N_{FRET} values was chosen in the plasma membrane area. Coexpression of transporter pairs tagged at the N or C terminus (Fig. 2*B*; hOCT2-CFP-C/hOCT2-YFP-C, bar *a*;, hOCT2-CFP-C/hOCT2-YFP-N, bar *b*; or hOCT2-CFP-N/hOCT2-YFP-N, bar *c*) in HEK293 cells showed enhanced plasma membrane fluorescence and robust N_{FRET} signals (0.180±0.007, *n*=6; 0.171±0.012, *n*=12; and 0.176±0.012, *n*=9, respectively; Fig. 2*B*), comparable with the values for CFP- and YFP-fused SERT, which were utilized as a positive control for transporter dimerization (ref. 26; 0.198±0.054, *n*=10; Fig. 2*B*, bar *f*). This confirms in living HEK293 cells the findings in mbSUS that hOCT2 forms oligomers. To exclude false-positive results, hOCT2-CFP-C or hOCT2-CFP-N was cotransfected with a Palm-myr-YFP construct, which leads to membrane localization of the YFP, thus generating a negative control directly. These N_{FRET} values (0.060±0.024, *n*=6; and 0.076±0.024, *n*=6; Fig. 2*B*, bars *d* and *e*, respectively) were significantly lower than those obtained for the transporter measurements in the plasma membrane and lie in the range of the background controls CFP and YFP (0.040±0.022, *n*=10; not shown). As expected, the strongest N_{FRET}

values were obtained for the positive control CFP-YFP fusion, where CFP and YFP were expressed as fusion protein (0.634±0.056, *n*=7; not shown; ref. 32). Interestingly, N_{FRET} values were similar when the transporter proteins were tagged at the N or C terminus.

Identification of the interaction domain with the mbSUS

To determine which domains are involved in the observed hOCT2-hOCT2 interactions, the mbSUS was again applied. As bait, the whole transporter protein was fused to the C-terminal part of the ubiquitin, while as prey, several different truncations of the hOCT2 were fused to the N-terminal part. These 5 truncated transporter proteins contained the first 50 (Fig. 3**,** *a*), 152 (Fig. 3, *b*), 169 (Fig. 3, *c*), 284 (Fig. 3, *d*), or 376 (Fig. 3, *e*) amino acids. These truncations were chosen in order to test whether the part of hOCT2 in proximity of the C terminus (Fig. 3, truncation *e*) or of the big intracellular loop (Fig. 3, truncation *d*) is involved in hOCT2-hOCT2 interaction. Screening the primary sequence of hOCT2 reveals 2 known dimerization motifs. The first is the noncovalent GxxxG motif at positions 159 to 163 in the second TMD, originally found in glycophorin A (33, 34). The second is a covalent dimerization motif formed by 6 cysteine residues in the large extracellular loop. Covalent dimerization mediated by disulfide bonds is known (*e.g.*, the tight junction protein occludin; ref. 35). Comparing these sequence regions of hOCT2 with other members of the OCT family, it is evident that these 2 motifs are highly conserved in all orthologs of the transporter independent of the species (see Supplemental Table S4). For this reason, truncations were designed such that truncation *c* does contain the glycine motif, and truncation *b* does not contain the glycine motif, while truncation *a* misses the extracellular loop containing the 6 cysteine residues (Fig. 3).

Only in the case of the shortest mutant (Fig. 3, truncation *a*), which only expressed the first 50 aa as prey protein, no growth of the yeasts on minimal medium was observed, indicating no interaction with the bait. Conversely, truncation *b*, which consists of the first 152 aa, including the first and part of the second TMDs and the big extracellular loop (Fig. 3), showed an interaction, suggesting that the interaction domain is localized within the first 152 aa. Thus, hOCT2-hOCT2 interaction involves the N terminus, the first and the second TMDs, and the big extracellular loop between them. Therefore, mainly the 6 cysteine residues of the extracellular loop, but not the glycine dimerization motif, may be involved in hOCT2-hOCT2 interaction.

In summary, on the basis of the mbSUS results, we suggest an essential role of the cysteine motif on the postulated big extracellular loop for oligomerization of hOCT2 and for the determination of its quaternary structure.

Western blot analysis

The role of the cysteine motif for oligomerization of hOCT2 has been further explored by comparing the molecular mass of hOCT2 in lysates of HEK293 cells stably expressing hOCT2 under reducing and nonreducing conditions. In Western blot analysis under reducing conditions using a monoclonal antibody against hOCT2, 2 transporter bands were detected: one band of ~55 kDa, probably corresponding to the monomeric nonglycosylated form, and a second band between 70 and 100 kDa, probably corresponding to the monomeric

glycosylated form of the transporter (Fig. 4, lane *a*). In fact, deglycosylation of the protein by PNGaseF treatment produced one major band of ~55 kDa, as described also for rbOCT2 (ref. 36; Fig. 4, lane *c*).

Performing the Western blot analysis under nonreducing conditions, the nonreduced transporter seems to shift, with 2 further bands with relative molecular mass of ~150 and >250 kDa, in addition to the 2 monomeric forms (Fig. 4, lane *b*). To exclude whether this behavior might be a result of the high-level transporter expression in stably transfected hOCT2-HEK293 cells, the same experiments were performed with human whole kidney lysates.

Also in this preparation, under reducing conditions, a major band at ~55 kDa and a second minor band between 70 and 100 kDa, analogous to what was seen in stably transfected hOCT2 cells, were observed (Fig. 5, lane *b*). Under nonreducing conditions, further bands with relative molecular mass of ~150 and > 250 kDa, in addition to the monomeric band at ~55 kDa, were detected (Fig. 5, lane *a*). In some experiments, further signals in proximity to the monomeric band could be observed, which may be attributed to the presence of different transporter forms, such as precursor forms, transporters at different glycosylation stages, or degradation products (not shown). Interestingly, under nonreducing conditions, no signal corresponding to the glycosylated monomer was detected. This fact is not surprising because of the tiny expression of glycosylated transporters observed under reducing conditions and suggests that glycosylated hOCT2 is present in the human kidney prevalently as an oligomer.

Since cysteines are involved in disulfide bridge formation, as an initial test for the existence of a functionally relevant disulfide bond in hOCT2, the transport of the fluorescent organic cation ASP$^+$ was measured after 10 min incubation with different concentrations of the reducing agent DTT. Brief incubation of living cells with micromolar concentrations of DTT has been already shown to prevent the formation of disulfide bonds on nascent and newly synthesized membrane proteins and to induce reduction of already folded and oxidized monomers, without influencing protein translation, translocation, and processing (37, 38). Under these conditions, the transport of ASP$^+$ was significantly reduced both in stably transfected hOCT2-HEK293 cells and in freshly isolated human PTs (Fig. 6), indicating the importance of disulfide bridges for full transport function. Incubation with 20 mM DTT did not significantly change the apparent affinity of hOCT2 for TEA$^+$ (log IC$_{50}$ −4.10±0.15 and −3.96±0.12 μM with or without incubation with DTT respectively; *n*=6 for every TEA$^+$ concentration tested, from 10^{-3} to 10^{-6} M; not shown).

Mutagenesis and functional measurements

Because the results of Western blot analysis under nonreducing conditions and the results of the mbSUS suggested the existence of a covalent dimerization motif, and since the ASP$^+$ transport in the presence of the reducing agent DTT was lower, suggesting the existence of functionally important disulfide bridges, we further focused on the 6 cysteine residues in the extracellular domain. To check whether one or more of these cysteines could be involved in the oligomerization of hOCT2, each of the cysteines of the big extracellular loop was individually mutated to alanine (mutants C51A, C63A, C89A, C103A, C122A, and C143A).

Furthermore, 2 control mutations of hOCT2 were created by mutating a glycine of the extracellular loop at position 120 to alanine (G120A) and a further cysteine residue at position 179 to alanine (C179A), which is not located in the hypothesized interaction domain. All mutated transporter constructs and the WT hOCT2 were individually transiently transfected into HEK293 cells.

Cross-linking experiments

The role of sulfhydryl groups in the hOCT2 oligomer formation was investigated in detail by cross-linking experiments with lysates from hOCT2-HEK293 using the homobifunctional maleimide cross-linker BM(PEG)$_2$ for conjugation between sulfhydryl groups. Western blot analysis of the BM(PEG)$_2$ cross-linked mutated transporters showed a band clearly <52 kDa, probably representing a precursor or a degradation product of the transporter (Fig. 7). Moreover, a band with an apparent molecular mass > 52 kDa, probably representing the nonglycosylated monomer, was also detected. More important, cross-linking of a single mutated hOCT2 still resulted in formation of high-molecular-mass complexes (at ~150 and >250 kDa) corresponding to what we observed under nonreducing conditions, suggesting that more than one cysteine residue is involved in the cross-linking of the transporter. Single transporter forms showed different band intensities depending on cross-linking efficiency. For example, in the lane containing the C179A hOCT2, a band between 72 and 95 kDa, not visible in the other preparations, is evident.

To test the hypothesis that more than one cysteine of the extracellular loop is necessary for oligomerization, combined mutants were created (C51A/C63A, C51A/C63A/C89A, C51A/ C63A/C89A/C103A, C51A/C63A/C89A/C103A/C122A, C51A/C63A/C89A/C103A/ C122A/C143A, and C51A/C143A). All transporters show 2 bands probably representing the nonglycosylated and glycosylated hOCT2 monomers (at ~55 and between 72 and 95 kDa, respectively). Again, cross-linking efficiency varied between the samples, resulting in different band intensities (Fig. 8). Only the mutants C51A/C63A/C89A/C103A/C122A/ C143A (Fig. 8, lane *g*), where all 6 loop cysteines were mutated, and C51A/C143A (Fig. 8, lane *h*), where the first and the last loop cysteines were mutated, never showed bands at higher molecular mass after cross-linking, suggesting that these 2 amino acids are essential for hOCT2 oligomerization.

Interestingly, functional studies 48 h after transfection showed a significantly lower transport of ASP[+] by each of the 6 extracellular loop single-cysteine mutants (C51A, C63A, C89A, C103A, C122A, and C143A), even though they could be still cross-linked to oligomers. The control mutation constructs G120A and G179A had similar transport rates of ASP[+] as the WT hOCT2 (Fig. 9).

To investigate the reason for the decreased ASP[+] transport by these cysteine mutants, their cellular distribution was investigated by fluorescence microscopy. To do this, the WT-, C51A-, C63A-, C89A-, C103A-, C122A-, C143A-, G120A-, and G179A-hOCT2 constructs were fused to GFP and transiently expressed in HeLa SS6 cells. At 24 h after transfection, the hOCT2-GFP-WT transporter and the transporters bearing control mutations G120A and C179A were mainly located in the plasma membrane. The majority of the 6 cysteine mutants (C51A, C63A, C89A, C103A, C122A, and C143A) remained in the cytosol,

suggesting that the mutation of only one of the loop cysteines strongly influences the trafficking of the transporter. Figure 10 shows the results obtained with WT-, C63A-, G120A-, and G179A-hOCT2. The GFP-tagged mutated transporter C63A remained in a perinuclear area, while the control mutants G120A and G179A showed a localization as in WT. This subcellular compartment does not correspond either to the ER or to the Golgi, since only less colocalization of the transporter-associated GFP signal with calnexin (an ER marker) or GM130 (a Golgi marker) was observed.

DISCUSSION

Homooligomer formation has been already described for several membrane transporters, *e.g.*, the Na^+-dependent neurotransmitter transporter (20). Within the SLC-transporter families, oligomerization was also shown for zinc transporter 3, a member of the SLC30A family (39), for the electrogenic SLC4 Na^+-HCO_3^- cotransporter NBCe1-A (40), and for human organic anion transporter 1 (hOAT1), a member of the SLC22A family (41), which also includes hOCT2. First hints for dimerization of organic cation transporters come from the work of Keller *et al.* (42). In a cell-free expression system, the researchers could show an interaction between rOCT1 monomers *in vitro*. In the present work, we investigated the ability of hOCT2 to form oligomeric complexes *in vivo* and also *in vitro*. In a first approach, we expressed hOCT2 protein molecules in yeast cells. The mbSUS is specialized for investigations of membrane proteins, since in this system, protein interactions take place in the plasma membrane, in contrast to usual 2-hybrid systems (22, 23). As depicted in Fig. 1, we showed that hOCT2 is able to interact with itself *in vivo*. Applying FRET technology, we confirmed this result from the mbSUS and got further evidence for the existence of oligomeric structures of hOCT2 proteins in the cell membrane. Since the same FRET intensities were obtained regardless of which end, N or C terminus, of the hOCT2 was tagged with the YFP or CFP (Fig. 2), and since energy transfer from the hOCT2-CFP to hOCT2-YFP occurs only if the distance is <50 Å, it can be concluded that in the quaternary end conformation, the N and C termini of the transporter oligomers in the plasma membrane are in proximity.

The results of the mbSUS experiments with the truncated hOCT2, to define the interaction domains responsible for homooligomer formation, suggest that the interaction domain is localized between aa 50 and 152 (Fig. 4). Here, a highly conserved dimerization motif is represented by the 6 cysteine residues in the extracellular loop. Covalent dimerization mediated by disulfide bonds is known, *e.g.*, for the transmembrane tight junction protein occludin (35). In proximity to these residues, in the second TMD (aa 159 to 163), a noncovalent GxxxG-dimerization motif originally found in glycophorin A (33, 34) is highly conserved in all orthologs of the transporter, independent of the species. However, this domain does not seem to be directly involved in the hOCT2 oligomerization, since an interaction in yeast cells could still be observed with mbSUS when expressing a truncated hOCT2 protein without the GxxxG motif as prey and the whole hOCT2 as bait.

Western blot analysis of cell lysates from hOCT2-HEK293 cells and from human kidney showed that under reducing conditions, 2 transporter bands at ~55 and between 70 and 100 kDa could be observed. Experiments with PNGase confirmed that these bands correspond to

the nonglycosylated and glycosylated hOCT2, respectively. Under nonreducing conditions, further bands at ~150 and >250 kDa were observed in both preparations, suggesting the presence of dimeric and also tetrameric transporter complexes. Notably, the postulated oligomeric forms of the transporter are not only a product of protein overexpression in the expression system, but are also present in human kidney tissue, which endogenously expresses hOCT2.

Incubation with DTT, which cleaves disulfide bridges, caused a significant decrease of ASP$^+$ transport in HEK293 cells stably expressing hOCT2 and also in isolated human PTs, implying that a disulfide bond is formed and can be reduced. The apparent affinity of hOCT2 for TEA$^+$ seems not to be changed under DTT incubation, excluding DTT effects on the binding pocket of hOCT2.

Cross-linking experiments showed that the disulfide linking of hOCT2 results in proteins with higher molecular mass, which could be a glycosylated dimer (150 kDa), and a glycosylated tetramer with a size clearly >250 kDa. However, since the antibody used in this study recognizes glycosylated better than nonglycosylated hOCT2 (our own data), we cannot exclude the formation of nonglycosylated oligomers. Because of the possible involvement of the extracellular loop cysteines in dimerization, we tested whether it is possible to cross-link the cysteines of the extracellular loop with the cell membrane-impermeant cross-linker BM(PEG)$_2$ both in cell lysates and also in intact hOCT2-overexpressing HEK293 cells. After BM(PEG)$_2$ treatment of intact cells and subsequent Western blot analysis, only the monomeric forms of the transporter were detected, showing that it was not possible to cross-link the extracellular cysteine residues (data not shown). We speculate that in the plasma membrane, the hOCT2 proteins are in end conformation, with the extracellular loop outside, and in this end-conformation quaternary structure, they do not expose any free sulfhydryl group that could react with the cross-linker. Similar data have been obtained by investigations of the cysteine accessibility in the hydrophilic cleft of hOCT2 (43). In that work, experiments aimed to precipitate the transporter with the membrane-impermeable maleimide-PEO2 biotin showed the inaccessibility for the loop cysteines (43).

From these experiments, we conclude that the hOCT2 forms stable dimers or higher oligomeric forms by covalent S-S bonds between monomeric subunits. In a next step, the role of the 6 loop cysteines for dimerization was investigated by performing single mutation of the 6 loop cysteine residues to alanine. Mutation of any single loop cysteine to alanine did not prevent the covalent binding between protein monomers to oligomers. However, transport measurements of the fluorescent organic cation ASP$^+$ showed that the mutation of one loop cysteine was sufficient to strongly diminish the transporter function, underlining the importance of these residues. These effects were specific, since control mutants (a cysteine outside of the loop and a noncysteine replacement in the loop) were still able to transport ASP$^+$ comparably to the WT hOCT2, showing that the loop cysteines have an essential relevance for protein conformation and function. To explain the decreased ASP$^+$ transport after mutation, immunofluorescence analysis of cellular distribution of GFP-tagged cysteine-mutant constructs were performed. These experiments showed that the mutated proteins accumulated in the cytosol in very large amounts, suggesting that the trafficking to

the plasma membrane was interrupted (Fig. 10). We assume that the proteins left the ER and the Golgi apparatus but were recognized as not correctly folded and sent to the degradation machinery or sequestrated in aggregosomes, explaining the plaque-like accumulation in the cytosol of overexpressing HeLa cells (Fig. 10). It is known that during protein synthesis, proteins associate with different chaperone systems of the ER to get the correct folding. On the basis of our results, one of these systems could be the binding to protein disulfide isomerases (PDIs), which catalyzes protein disulfide bond formation, reduction, or isomerization (44). In fact, we found PDIs to be a direct interaction partner of hOCT2 in the mbSUS screening (unpublished results). When the 6 single loop cysteines are mutated, PDI is apparently no more able to efficiently link free sulfhydryl groups within the loop or between 2 loops of hOCT2 monomers, which are synthesized on the same polyribosome. The mutated hOCT2 proteins probably left the protein-sorting machinery as misfolded proteins and were degraded. Only correctly folded hOCT2 proteins will be efficiently transported to the plasma membrane. Moreover, since only the hOCT2 without any loop cysteine and the double mutant C51/143A could not be cross-linked, we suggest that more than one cysteine is necessary to form oligomers. However, it cannot be excluded that additional nonloop cysteines are involved in oligomer formation and/or stabilization. A 3-dimensional model of OCT structure in the plasma membrane suggests that the 12 TMDs form a ring structure in the plasma membrane (45). Here, we show that hOCT2 forms oligomers and, because of the FRET signals, suggest that the C and N termini are in proximity (TMDs 1 and 12) not only in the monomeric but also in the oligomeric form of the transporter. In the case of a dimeric protein, it can be speculated that 2 monomers face each other in the plasma membrane with the first 2 TMDs and that the 2 cysteines (aa 51 and 143) near the plasma membrane play an essential role in oligomerization.

Given that all mutants (except control mutants) are not expressed or expressed only at low levels in the plasma membrane, we do not know how important a dimeric or oligomeric structure is for substrate binding and transporter function.

In summary, in this work we demonstrate that hOCT2 is able to oligomerize *in vivo* and *in vitro*. Oligomerization takes place not only in cell culture systems, but also in human PTs. The extracellular loop seems to be a determinant in oligomer formation. In oligomers, the carboxyl and amino termini of the oligomer-building monomers are in proximity. The single cysteines of the extracellular loop are important to allow the correct folding, assembly, and plasma membrane insertion of hOCT2.

Supplementary Material

Refer to Web version on PubMed Central for supplementary material.

Acknowledgments

Abbreviations

ASP⁺	4-(4-(dimethylamino)styryl)-*N*-methylpyridinium
BM(PEG)₂	1,8-*bis*-(maleimido)diethylene glycol
Cub	C-terminal ubiquitin
DTT	dithiothreitol
ER	endoplasmic reticulum
FRET	fluorescence resonance energy transfer
hOCT2	human organic cation transporter 2
mbSUS	mating-based split-ubiquitin system
Nub	N-terminal ubiquitin
PDI	protein disulfide isomerase
PLV	protein A-LexA-VP16
PT	proximal tubule
SERT	serotonin transporter
SNP	single-nucleotide polymorphism
TEA⁺	tetraethylammonium
TMD	transmembrane domain
USP	ubiquitin-specific protease

REFERENCES

1. Koepsell H, Schmitt BM, Gorboulev V. Organic cation transporters. Rev. Physiol. Biochem. Pharmacol. 2003; 150:36–90. [PubMed: 12827517]

2. Taubert D, Grimberg G, Stenzel W, Schomig E. Identification of the endogenous key substrates of the human organic cation transporter OCT2 and their implication in function of dopaminergic neurons. PLoS ONE. 2007; 2:e385. [PubMed: 17460754]

3. Ogasawara M, Yamauchi K, Satoh Y, Yamaji R, Inui K, Jonker JW, Schinkel AH, Maeyama K. Recent advances in molecular pharmacology of the histamine systems: organic cation transporters as a histamine transporter and histamine metabolism. J. Pharmacol. Sci. 2006; 101:24–30. [PubMed: 16648665]

4. Kimura N, Okuda M, Inui K. Metformin transport by renal basolateral organic cation transporter hOCT2. Pharm. Res. 2005; 22:255–259. [PubMed: 15783073]

5. Kimura N, Masuda S, Tanihara Y, Ueo H, Okuda M, Katsura T, Inui K. Metformin is a superior substrate for renal organic cation transporter OCT2 rather than hepatic OCT1. Drug Metab. Pharmacokinet. 2005; 20:379–386. [PubMed: 16272756]

6. Ciarimboli G, Deuster D, Knief A, Sperling M, Holtkamp M, Edemir B, Pavenstadt H, Lanvers-Kaminsky C, Am Zehnhoff-Dinnesen A, Schinkel AH, Koepsell H, Jurgens H, Schlatter E. Organic cation transporter 2 mediates cisplatin-induced oto- and nephrotoxicity and is a target for protective interventions. Am. J. Pathol. 2010; 176:1169–1180. [PubMed: 20110413]

7. Ciarimboli G, Ludwig T, Lang D, Pavenstadt H, Koepsell H, Piechota HJ, Haier J, Jaehde U, Zisowsky J, Schlatter E. Cisplatin nephrotoxicity is critically mediated via the human organic cation transporter 2. Am. J. Pathol. 2005; 167:1477–1484. [PubMed: 16314463]

8. Yonezawa A, Masuda S, Yokoo S, Katsura T, Inui K. Cisplatin and oxaliplatin, but not carboplatin and nedaplatin, are substrates for human organic cation transporters (SLC22A1–3 and multidrug and toxin extrusion family). J. Pharmacol. Exp. Ther. 2006; 319:879–886. [PubMed: 16914559]

9. More SS, Li S, Yee SW, Chen L, Xu Z, Jablons DM, Giacomini KM. Organic cation transporters modulate the uptake and cytotoxicity of picoplatin, a third-generation platinum analogue. Mol. Cancer Ther. 2010; 9:1058–1069. [PubMed: 20371711]

10. Ciarimboli G, Holle SK, Vollenbroker B, Hagos Y, Reuter S, Burckhardt G, Bierer S, Herrmann E, Pavenstadt H, Rossi R, Kleta R, Schlatter E. New clues for nephrotoxicity induced by ifosfamide: preferential renal uptake via the human organic cation transporter 2. Mol. Pharm. 2011; 8:270–279. [PubMed: 21077648]

11. Chen Y, Zhang S, Sorani M, Giacomini KM. Transport of paraquat by human organic cation transporters and multidrug and toxic compound extrusion family. J. Pharmacol. Exp. Ther. 2007; 322:695–700. [PubMed: 17495125]

12. Motohashi H, Sakurai Y, Saito H, Masuda S, Urakami Y, Goto M, Fukatsu A, Ogawa O, Inui KK. Gene expression levels and immunolocalization of organic ion transporters in the human kidney. J. Am. Soc. Nephrol. 2002; 13:866–874. [PubMed: 11912245]

13. Aperia AC. Intrarenal dopamine: a key signal in the interactive regulation of sodium metabolism. Annu. Rev. Physiol. 2000; 62:621–647. [PubMed: 10845105]

14. Lazar A, Zimmermann T, Koch W, Grundemann D, Schomig A, Kastrati A, Schomig E. Lower prevalence of the OCT2 Ser270 allele in patients with essential hypertension. Clin. Exp. Hypertens. 2006; 28:645–653. [PubMed: 17060063]

15. Sallinen R, Kaunisto MA, Forsblom C, Thomas M, Fagerudd J, Pettersson-Fernholm K, Groop PH, Wessman M. Association of the SLC22A1, SLC22A2, and SLC22A3 genes encoding organic cation transporters with diabetic nephropathy and hypertension. Ann. Med. 2010; 42:296–304. [PubMed: 20429798]

16. Neuhoff S, Ungell AL, Zamora I, Artursson P. pH-dependent bidirectional transport of weakly basic drugs across Caco-2 monolayers: implications for drug-drug interactions. Pharm. Res. 2003; 20:1141–1148. [PubMed: 12948010]

17. Busch AE, Karbach U, Miska D, Gorboulev V, Akhoundova A, Volk C, Arndt P, Ulzheimer JC, Sonders MS, Baumann C, Waldegger S, Lang F, Koepsell H. Human neurons express the polyspecific cation transporter hOCT2, which translocates monoamine neurotransmitters, amantadine, and memantine. Mol. Pharmacol. 1998; 54:342–352. [PubMed: 9687576]

18. Ciarimboli G, Schlatter E. Regulation of organic cation transport. Pflügers Arch. 2005; 449:423–441. [PubMed: 15688244]

19. Ellgaard L, Helenius A. Quality control in the endoplasmic reticulum. Nat. Rev. Mol. Cell. Biol. 2003; 4:181–191. [PubMed: 12612637]

20. Sitte HH, Farhan H, Javitch JA. Sodium-dependent neurotransmitter transporters: oligomerization as a determinant of transporter function and trafficking. Mol. Interv. 2004; 4:38–47. [PubMed: 14993475]

21. Biermann J, Lang D, Gorboulev V, Koepsell H, Sindic A, Schroter R, Zvirbliene A, Pavenstadt H, Schlatter E, Ciarimboli G. Characterization of regulatory mechanisms and states of human organic cation transporter 2. Am. J. Physiol. Cell Physiol. 2006; 290:C1521–C1531. [PubMed: 16394027]

22. Grefen C, Stadele K, Ruzicka K, Obrdlik P, Harter K, Horak J. Subcellular localization and in vivo interactions of the *Arabidopsis thaliana* ethylene receptor family members. Mol. Plant. 2008; 1:308–320. [PubMed: 19825542]

23. Grefen C, Lalonde S, Obrdlik P. Split-ubiquitin system for identifying protein-protein interactions in membrane and full-length proteins. Curr. Protoc. Neurosci. 2007; 41:5.27.1–5.27.41.

24. Xia Z, Liu Y. Reliable and global measurement of fluorescence resonance energy transfer using fluorescence microscopes. Biophys. J. 2001; 81:2395–2402. [PubMed: 11566809]

25. Feige JN, Sage D, Wahli W, Desvergne B, Gelman L. PixFRET, an ImageJ plug-in for FRET calculation that can accommodate variations in spectral bleed-throughs. Microsc. Res. Tech. 2005; 68:51–58. [PubMed: 16208719]

26. Schmid JA, Scholze P, Kudlacek O, Freissmuth M, Singer EA, Sitte HH. Oligomerization of the human serotonin transporter and of the rat GABA transporter 1 visualized by fluorescence

resonance energy transfer microscopy in living cells. J. Biol. Chem. 2001; 276:3805–3810. [PubMed: 11071889]

27. Pietig G, Mehrens T, Hirsch JR, Cetinkaya I, Piechota H, Schlatter E. Properties and regulation of organic cation transport in freshly isolated human proximal tubules. J. Biol. Chem. 2001; 276:33741–33746. [PubMed: 11447227]

28. Pietruck F, Ullrich KJ. Transport interactions of different organic cations during their excretion by the intact rat kidney. Kidney Int. 1995; 47:1647–1657. [PubMed: 7643534]

29. Rohlicek V, Ullrich KJ. Simple device for continuous measurement of fluorescent anions and cations in the rat kidney in situ. Ren. Physiol. Biochem. 1994; 17:57–61. [PubMed: 7513899]

30. Wilde S, Schlatter E, Koepsell H, Edemir B, Reuter S, Pavenstadt H, Neugebauer U, Schroter R, Brast S, Ciarimboli G. Calmodulin-associated post-translational regulation of rat organic cation transporter 2 in the kidney is gender dependent. Cell. Mol. Life Sci. 2009; 66:1729–1740. [PubMed: 19330287]

31. Ciarimboli G, Koepsell H, Iordanova M, Gorboulev V, Dürner B, Lang D, Edemir B, Schröter R, van Le T, Schlatter E. Individual PKC-phosphorylation sites in organic cation transporter 1 determine substrate selectivity and transport regulation. J. Am. Soc. Nephrol. 2005; 16:1562–1570. [PubMed: 15829703]

32. Just H, Sitte HH, Schmid JA, Freissmuth M, Kudlacek O. Identification of an additional interaction domain in transmembrane domains 11 and 12 that supports oligomer formation in the human serotonin transporter. J. Biol. Chem. 2004; 279:6650–6657. [PubMed: 14660642]

33. Lemmon MA, Flanagan JM, Treutlein HR, Zhang J, Engelman DM. Sequence specificity in the dimerization of transmembrane alpha-helices. Biochemistry. 1992; 31:12719–12725. [PubMed: 1463743]

34. Lemmon MA, Flanagan JM, Hunt JF, Adair BD, Bormann BJ, Dempsey CE, Engelman DM. Glycophorin A dimerization is driven by specific interactions between transmembrane alpha-helices. J. Biol. Chem. 1992; 267:7683–7689. [PubMed: 1560003]

35. Walter JK, Castro V, Voss M, Gast K, Rueckert C, Piontek J, Blasig IE. Redox-sensitivity of the dimerization of occludin. Cell. Mol. Life Sci. 2009; 66:3655–3662. [PubMed: 19756380]

36. Pelis RM, Suhre WM, Wright SH. Functional influence of N-glycosylation in OCT2-mediated tetraethylammonium transport. Am. J. Physiol. Renal Physiol. 2006; 290:F1118–F1126. [PubMed: 16368738]

37. Tatu U, Braakman I, Helenius A. Membrane glycoprotein folding, oligomerization and intracellular transport: effects of dithiothreitol in living cells. EMBO J. 1993; 12:2151–2157. [PubMed: 8491203]

38. Braakman I, Helenius J, Helenius A. Manipulating disulfide bond formation and protein folding in the endoplasmic reticulum. EMBO J. 1992; 11:1717–1722. [PubMed: 1582407]

39. Salazar G, Falcon-Perez JM, Harrison R, Faundez V. SLC30A3 (ZnT3) oligomerization by dityrosine bonds regulates its subcellular localization and metal transport capacity. PLoS ONE. 2009; 4:e5896. [PubMed: 19521526]

40. Kao L, Sassani P, Azimov R, Pushkin A, Abuladze N, Peti-Peterdi J, Liu W, Newman D, Kurtz I. Oligomeric structure and minimal functional unit of the electrogenic sodium bicarbonate cotransporter NBCe1-A. J. Biol. Chem. 2008; 283:26782–26794. [PubMed: 18658147]

41. Hong M, Xu W, Yoshida T, Tanaka K, Wolff DJ, Zhou F, Inouye M, You G. Human organic anion transporter hOAT1 forms homooligomers. J. Biol. Chem. 2005; 280:32285–32290. [PubMed: 16046403]

42. Keller T, Schwarz D, Bernhard F, Dotsch V, Hunte C, Gorboulev V, Koepsell H. Cell free expression and functional reconstitution of eukaryotic drug transporters. Biochemistry. 2008; 47:4552–4564. [PubMed: 18361503]

43. Pelis RM, Zhang X, Dangprapai Y, Wright SH. Cysteine accessibility in the hydrophilic cleft of the human organic cation transporter 2. J. Biol. Chem. 2006; 281:35272–35280. [PubMed: 16990275]

44. Gilbert HF. Protein disulfide isomerase and assisted protein folding. J. Biol. Chem. 1997; 272:29399–29402. [PubMed: 9367991]

45. Gorbunov D, Gorboulev V, Shatskaya N, Mueller T, Bamberg E, Friedrich T, Koepsell H. High-affinity cation binding to organic cation transporter 1 induces movement of helix 11 and blocks transport after mutations in a modeled interaction domain between two helices. Mol. Pharmacol. 2008; 73:50–61. [PubMed: 17940192]
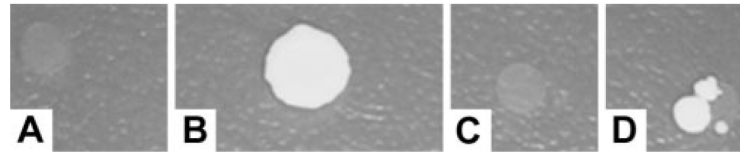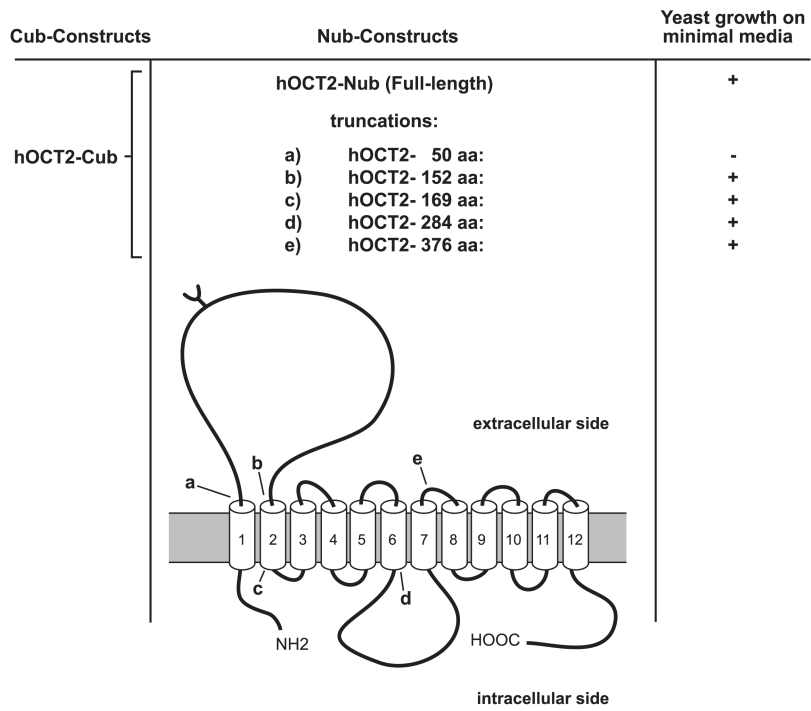
Figure 1.
hOCT2-expressing yeast cells grown on minimal medium in the split ubiquitin system (mbSUS). Reporter gene activation was shown as growth of yeast cells on minimal medium without adenine and histidine. *A–C*) Negative controls hOCT2-Cub with an empty NubG vector (*A*) and hOCT2-Cub with VATPase-NubG (*C*) showed no yeast growth; positive control showed strong growth of hOCT2-Cub with WT Nub-expressing cells (*B*). *D*) Reassociation of ubiquitin as a hint for protein interaction resulting in growth was shown for hOCT2-Cub (bait) with hOCT2-NubG (prey)-expressing yeast cells (*D*).
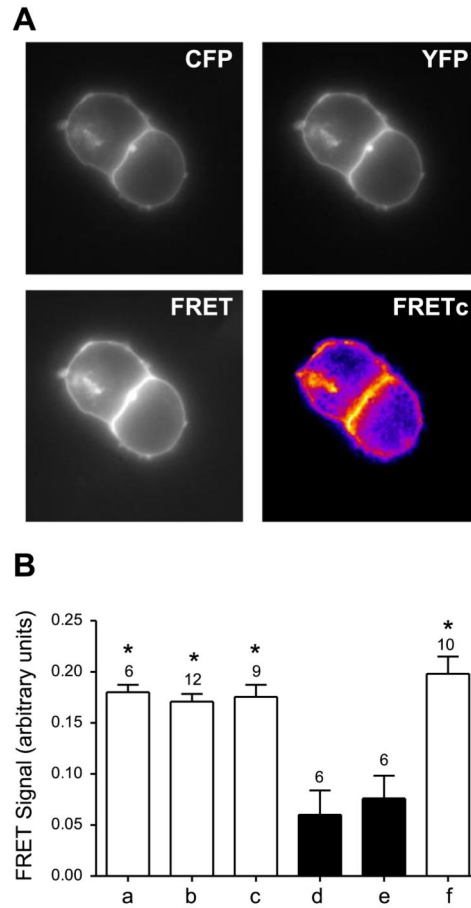
Figure 2.
Interaction between hOCT2 and hOCT2 visualized by FRET microscopy. *A*) High
magnification of HEK293 cells transfected with hOCT2-YFP and hOCT2-CFP (top left
panel, CFP channel; top right panel, YFP channel; bottom left panel, FRET channel; bottom
right panel, corrected FRET channel). FRETc images are displayed using pseudocolors. *B*)
Results of FRET analysis in living HEK293 cells expressing hOCT2-CFP and hOCT2-YFP
protein pairs tagged at the C or N terminus (bar *a*, hOCT2-CFP-C and hOCT2-YFP-C; bar
b, hOCT2-CFP-C and hOCT2-YFP-N; bar *c*, hOCT2-CFP-N and hOCT2-YFP-N). Positive-
control experiments included cells transfected with a CFP-YFP tandem construct (not
shown) and cells coexpressing SERT-CFP and SERT-YFP (bar *f*); negative controls
included cells cotransfected with CFP and YFP (not shown) and cells coexpressing PALM-
MYR-YFP and hOCT2-CFP (bar *d*, hOCT2-CFP-C; bar *e*, hOCT2-CFP-N). Intensity of
FRET was measured for the different combinations of CFP/YFP pairs and expressed as
normalized FRET values, as described in Materials and Methods. Values are means ± SE;
numbers above bars denote number of monolayers. *$P < 0.05$ *vs.* negative controls;
ANOVA.

Figure 3.
Truncation strategy of hOCT2 and results of mbSUS with truncated transporter.
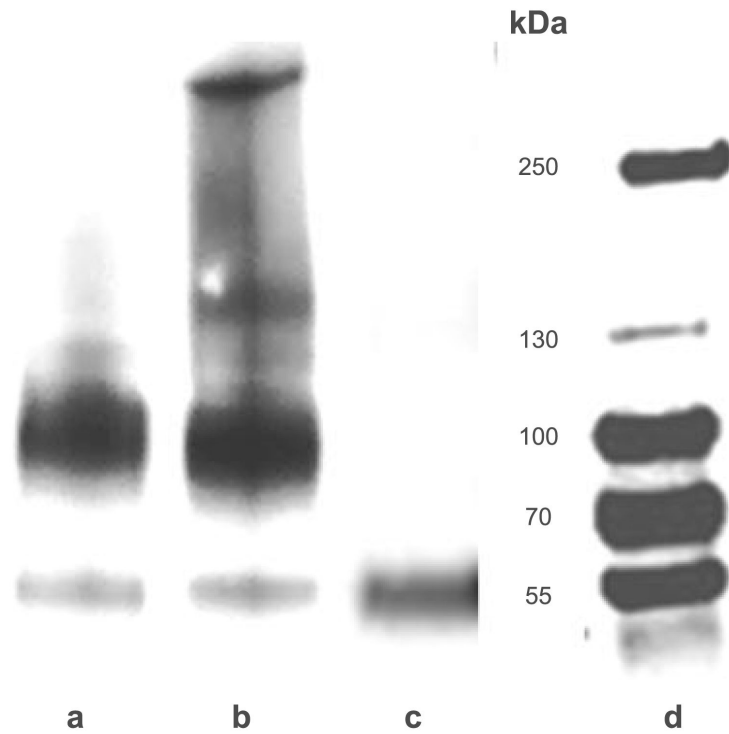
Figure 4.
Western blot analysis of hOCT2-HEK cell lysates. Representative experiments with hOCT2-HEK cell lysates under reducing conditions (lane *a*); under nonreducing conditions (lane *b*), and after pNGASE treatment (lane *c*), along with molecular mass markers (lane *d*). hOCT2 proteins were detected with an anti-hOCT2 antibody, which recognizes an epitope of the extracellular loop. Each experiment was repeated   3 times with independent cell preparations resulting in qualitatively similar results.
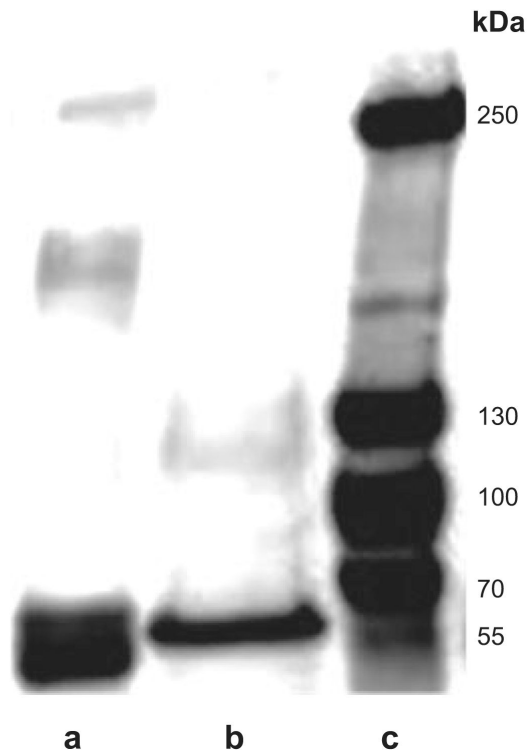
Figure 5.
Western blot analysis of human kidney lysates. Representative experiments with human kidney lysates under nonreducing conditions (lane *a*) and under reducing conditions (lane *b*), along with molecular mass markers (lane *c*). hOCT2 proteins were detected with an anti-hOCT2 antibody, which recognizes an epitope of the extracellular loop. Each experiment was repeated   3 times in independent human kidney preparations, resulting in qualitatively similar results.
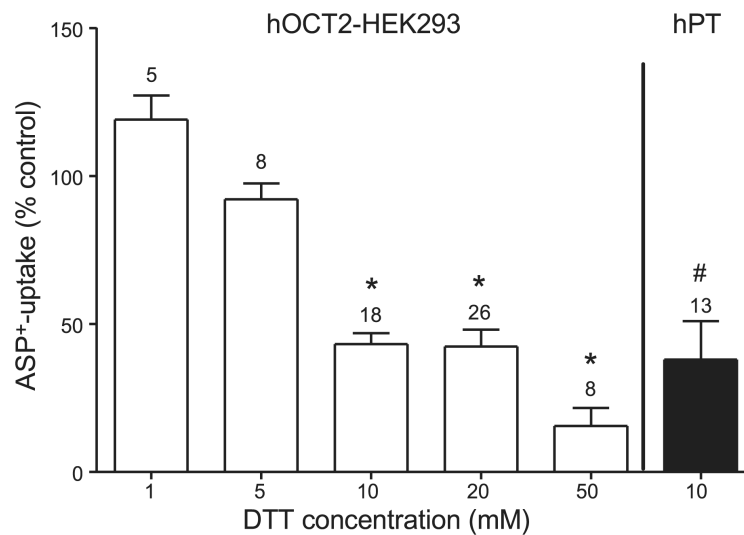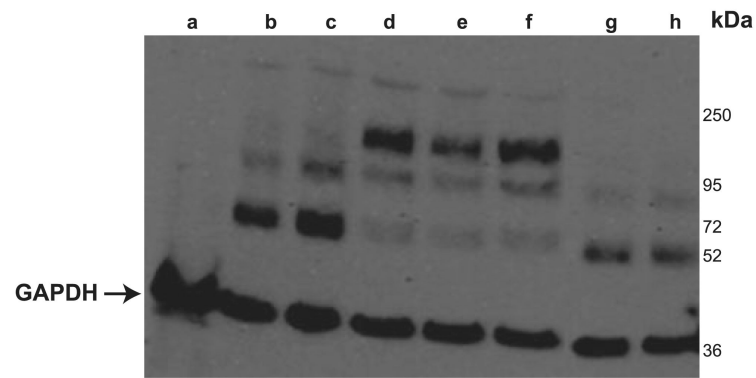
Figure 6.
Effect of 10 min incubation with the reducing agent DTT at different concentrations in hOCT2-expressing cells (open bars) and in freshly isolated S3 segments of PTs from human kidneys (hPT; solid bar). Data are presented as means ± SE; numbers above bars indicate number of cell preparations or human tubules used for each group. $*P < 0.05$ *vs.* control experiments in the presence of ASP^+ only or together with 1 or 5 mM DTT; ANOVA. $^{\#}P < 0.05$ *vs.* control experiments in the presence of ASP^+ only; unpaired *t* test.
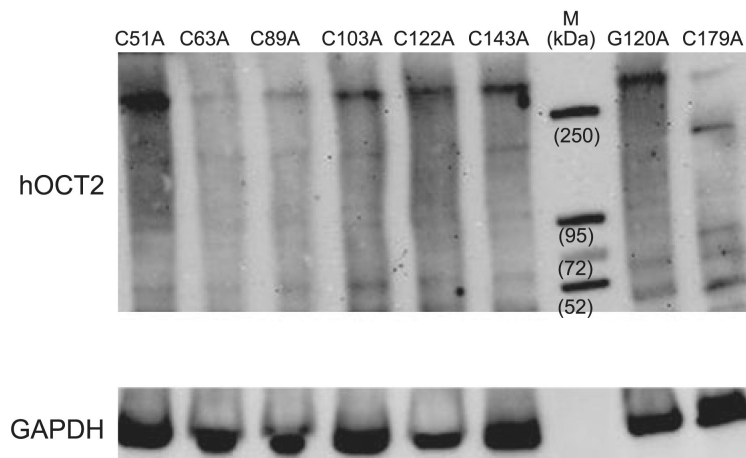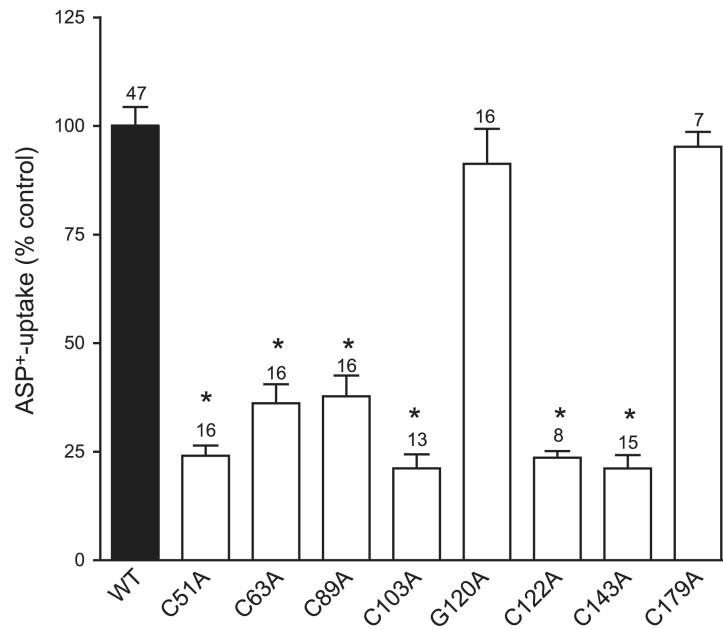
Figure 7.
Western blot analysis of HEK cell lysates cross-linked with BM(PEG)$_2$. Western blot analysis shows no difference after cross-linking in band pattern of the hOCT2 transporter bearing control mutations G120A and C179A compared with transporters, where single loop cysteines were mutated to alanine. M indicates molecular mass markers. hOCT2 proteins were detected with an anti-hOCT2 antibody, which recognizes an epitope of the extracellular loop. Bottom panel shows GAPDH signals of the lysates. Each experiment was repeated 3 times with independent cell preparations, resulting in qualitatively similar results.
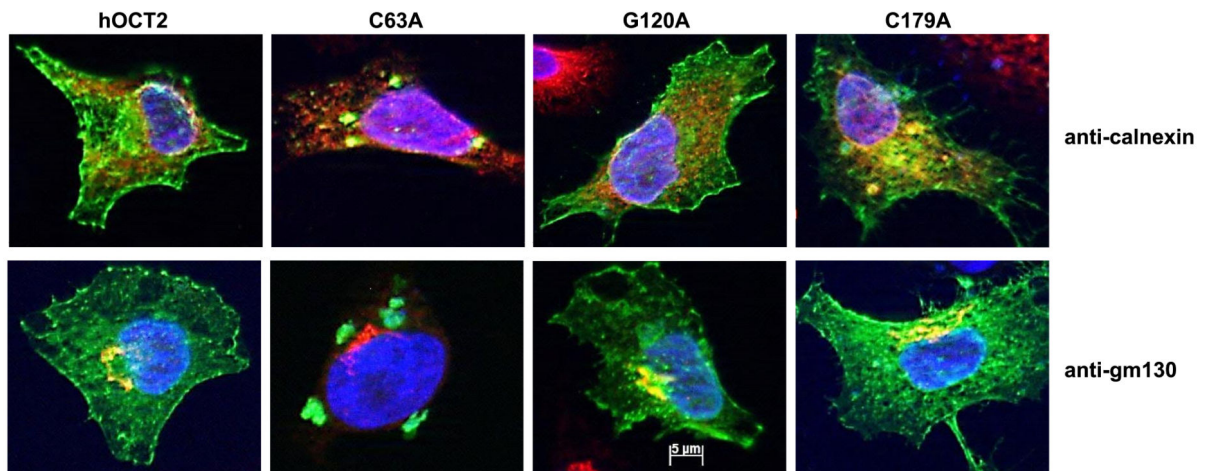
Figure 8.
Western blot analysis of HEK293 cells transfected or not (lane *a*) with WT hOCT2 (lane *b*) or multiple cysteine mutants (lane *c*, C51A/C63A; lane *d*, C51A/C63A/C89A; lane *e*, C51A/C63A/C89A/C103A; lane *f*, C51A/C63A/C89A/C103A/C122A; lane *g*, C51A/C63A/C89A/C103A/C122A/C143A; lane *h*, C51A/C143A). Only the mutants where all cysteines or the first and the last cysteines of the extracellular loop were mutated to alanine did not form any oligomer (lanes *g* and *h*). Arrow indicates GAPDH signals of the lysates. Each experiment was repeated 3 times with independent cell preparations, resulting in qualitatively similar results.

Figure 9.

ASP[+] uptake measurements of HEK cells transfected with WT hOCT2, or with hOCT2 mutants, where every single cysteine of the extracellular loop was substituted by alanine, or with 2 hOCT2 control mutants, where a glycine of the extracellular loop (G120) or a nonloop cysteine (C179) was mutated to alanine. Every mutation of the single cysteine of the extracellular loop led to a significant decrease in the transport of the model organic cation ASP[+]. Control mutants show similar transport function as the WT hOCT2. Data are presented as means ± SE. Numbers above bars indicate number of cell preparations used for each group. *$P < 005$ *vs*. WT hOCT2 control (set to 100%).

Figure 10.
Immunofluorescence of HeLa SS6 cells transfected with WT hOCT2 tagged with GFP, or with hOCT2-GFP mutants, where every single cysteine of the extracellular loop was substituted by alanine, or with 2 hOCT2-GFP control mutants, where a glycine of the extracellular loop (G120) or a nonloop cysteine (C179) was mutated to alanine. Cellular distribution of the hOCT2-GFP (in green) in the WT hOCT2-GFP, control hOCT2-GFP mutants, and the C63A-hOCT2-GFP mutant is shown. Golgi apparatus (anti-GM30) or ER (anti-calnexin) is labeled in red. Nuclei are labeled with DAPI (blue). Mutation of one single loop cysteine (C63A) led to an incorrect trafficking of the transporter, which is not, or only to a minor extent, expressed in plasma membrane, in contrast with what is observed in WT hOCT2 or the two hOCT2-bearing control mutation-expressing HeLa SS6 cells. Cysteine-mutated hOCT2 accumulates in a cytosolic compartment (plaques) that is not strictly colocalized with ER or Golgi.